Ceria Nanoparticles Synthesized With Aminocaproic Acid for the Treatment of Subarachnoid Hemorrhage

Han-Gil Jeong, MD, MSc; Bong Geun Cha, MSc; Dong-Wan Kang, MD; Do Yeon Kim, MD; Seul Ki Ki, BS; Song I. Kim, MS; Ju hee Han, BS; Wookjin Yang, MD; Chi Kyung Kim, MD, PhD; Jaeyun Kim, PhD; Seung-Hoon Lee, MD, PhD

Background and Purpose—Despite early aneurysm repair and aggressive management for complications, subarachnoid hemorrhage (SAH) results in at least 25% mortality rate and 50% persistent neurological deficit. We investigated whether ceria nanoparticles which have potent antioxidative activities can protect against subarachnoid hemorrhage via attenuating fatal brain injuries.

Methods—Uniform, 3 nm, water-dispersed ceria nanoparticles were prepared from short sol-gel reaction of cerium (III) ions with aminocaproic acid in aqueous phase. SAH was induced by endovascular perforation of middle cerebral artery of rats. A single dose of ceria nanoparticles (0.5 mg Ce/kg) or saline control was randomly administered intravenously at an hour post-SAH. Neuronal death, macrophage infiltration, SAH grade, and brain edema were evaluated at 72 hours. Mortality and neurological function were assessed for 14 days.

Results—The obtained ceria nanoparticles with high Ce^{3+} to Ce^{4+} ratio demonstrated potent antioxidative, cytoprotective, and anti-inflammatory activities in vitro. In rodent SAH models, the severity of hemorrhage was comparable between the ceria nanoparticles- and saline-treated groups. However, ceria nanoparticles significantly reduced neuronal death, macrophage infiltration, and brain edema after SAH. Ceria nanoparticles successfully improved survival rates (88.2% in the ceria nanoparticles group versus 21.1% in the control group; $P<0.001$) and neurological outcomes (modified Garcia score: 12.1±0.5 in the ceria nanoparticles group versus 4.4±0.5 in the control group; $P<0.001$) of the animals with SAH.

Conclusions—Ceria nanoparticles, totally synthesized in aqueous phase using aminocaproic acid, demonstrated promising results against SAH via potent antioxidative, neuroprotective and anti-inflammatory activities. Given the obvious limitations of current therapies for SAH, ceria nanoparticles can be a potential therapeutic agent which might result in a paradigm shift in SAH treatment.

Visual Overview—An online visual overview is available for this article. **(*Stroke*. 2018;49:3030-3038. DOI: 10.1161/STROKEAHA.118.022631.)**

Keywords: nanomedicine ■ neuroprotective agents ■ reactive oxygen species ■ stroke ■ subarachnoid hemorrhage

Subarachnoid hemorrhage (SAH), largely caused by rupture of cerebral aneurysm, is the most devastating type of stroke with a mortality rate up to 57% at 6 months and about 10% of patients even die before hospital arrival.[1,2] SAH tends to occur in younger population than other types of stroke, which results in a greater loss of productive life.[3] The recommended therapies in the guidelines are early aneurysm repair and oral nimodipine, but they only prevent rebleeding or delayed ischemia with modest efficacy.[4,5] There is currently no clinically effective therapeutic agent that directly rescue the fatal brain injuries from SAH.[4]

Reactive oxygen species (ROS) are excessively produced early after SAH and play a critical role in massive neuronal damages and inflammatory responses, resulting in irreversible brain injuries and poor clinical outcome.[6–9] Early brain injuries after SAH are activated by acute global ischemia and toxic-inflammatory reaction of blood products.[10] When aneurysms rupture and the blood pours into the subarachnoid space, intracranial pressure rises rapidly and cerebral ischemia is induced, resulting in mitochondrial dysfunction and bursts of ROS production such as superoxide anions.[11–14] In addition, hemoglobin and free heme produce a large amount of free

Received June 23, 2018; final revision received September 12, 2018; accepted September 25, 2018.

From the Laboratory of Innovative Nanotechnology, Biomedical Research Institute and Department of Neurology, Seoul National University Hospital, Republic of Korea (H.-G.J., D.-W.K., D.Y.K., S.K.K., S.I.K., J.h.H., W.Y., C.K.K., S.-H.L.); Korean Cerebrovascular Research Institute, Seoul (H.-G.J., D.-W.K., D.Y.K., S.K.K., S.I.K., J.h.H., W.Y., C.K.K., S.-H.L.); School of Chemical Engineering (B.G.C., J.K.), Department of Health Sciences and Technology, Samsung Advanced Institute for Health Science & Technology (SAIHST) (J.K.), and Biomedical Institute for Convergence (BICS) (J.K.), Sungkyunkwan University (SKKU), Suwon, Republic of Korea; Department of Neurology, Korea University Guro Hospital and Korea University College of Medicine, Seoul (C.K.K.); and Center for Nanoparticle Research, Institute for Basic Science (IBS), Seoul, Republic of Korea (S.-H.L.).

The online-only Data Supplement is available with this article at https://www.ahajournals.org/doi/suppl/10.1161/STROKEAHA.118.022631.

Correspondence to Seung-Hoon Lee, MD, PhD, Department of Neurology, Seoul National University Hospital, 101 Daehak-ro, Jongro-gu, Seoul 03080, Republic of Korea. Email sb0516@snu.ac.kr

radicals in the subarachnoid space through autoxidation and the Fenton reaction.[15,16] However, there is currently no clinically effective free radical scavengers targeting early brain damages from these reactions, because conventional antioxidants are not powerful enough to rapidly remove excessive ROS in SAH.

Cerium oxide nanoparticle (CeNP) is a potent and versatile ROS scavenger.[17–19] Cerium oxide has both 3+ and 4+ oxidation states at nanoscale and redox cycling between the 2 states enables autocatalytic, self-regenerative ROS scavenging activities.[19] CeNP has superoxide dismutase mimetic, catalase mimetic, and hydroxyl radical scavenging activities in a single component.[18,20,21] Because of high surface-to-volume ratio and oxygen vacancies at nanoscale, CeNP has innumerable action sites for scavenging ROS.[22] In the present study, we used the aqueous phase synthesis of CeNPs using aminocaproic acid as a surface modifier. This method resulted in CeNPs with a high Ce^{3+} to Ce^{4+} ratio which enhances their antioxidative and cytoprotective properties. Finally, we conducted a randomized animal trial to investigate whether free radical scavenging therapy using CeNPs reduces mortality and improves neurological outcomes in SAH.

Methods

The data that support the findings of this study are available from the corresponding author on reasonable request.

Synthesis of Biocompatible, Aminocaproic Acid-CeNPs

To synthesize discrete 3 nm CeNPs in aqueous phase, 10 mmol aminocaproic acid (Sigma-Aldrich Inc, St. Louis, MO) was dissolved in 60 mL of deionized water, and the mixture was heated to 95°C in air under magnetic stirring, and 70 mL of HCl (37% [v/v]; Duksan, South Korea) was added thereto. Cerium(III) nitrate hexahydrate ($Ce[NO_3]_3{\cdot}6H_2O$; 2.5 mmol; Alfa Aesar, Tewksbury, MA) was dissolved in 50 mL of deionized water at room temperature. Then, an aqueous solution of cerium(III) nitrate was added to the solution with aminocaproic acid. The reaction mixture was allowed to react for 1 minute and was cooled to 25°C. Surface Pegylation of CeNPs was achieved by mixing a CeNPs solution containing 20 mg of cerium ions with 500 mg of methoxy-polyethylene glycol succinimidyl glutarate (molecular weight = 5000; SunBio, South Korea) dissolved in 40 mL of ethanol. The mixture was stirred overnight at room temperature to induce the formation of covalent bonds between the amine groups of aminocaproic acid and the succinimidyl groups of polyethylene glycol. The resulting biocompatible, aminocaproic acid (BA)-CeNPs were washed 3× with acetone and dispersed in deionized water. For preparing dye-labeled BA-CeNPs, 13 mg of fluorescein isothiocyanate or 18 mg of rhodamine isothiocyanate were mixed with BA-CeNPs and reacted on rotator overnight at dark condition.

Physicochemical Characteristics of BA-CeNPs

The size and morphology of CeNPs were analyzed using transmission electron microscopy (200 kV; JEM-2100f, JEOL, Japan). X-ray diffraction patterns of the samples were obtained using a diffractometer (D/Max-3C; Rigaku, Japan). X-ray photoelectron spectroscopy analysis was performed using the Escalab 220i-XL (VG Scientific Instrument). Thermogravimetric analysis was performed using the Q50 (TA Instruments, New Castle, DE). Elemental analysis to measure concentration of nanoparticles was performed using an inductively coupled plasma mass spectrometer (ICP-MS; PerkinElmer).

Intracellular Uptake of BA-CeNPs

RAW264.7 cells were cultured in a 6-well plate and incubated with fluorescein isothiocyanate conjugated BA-CeNPs. Cells were collected into fluorescence-activated cell-sorting tubes. Using the BD FACSCalibur (BD Bioscience, San Jose, CA), we obtained relative optical densities of cells that absorbed the fluorescein isothiocyanate conjugated particles at various time points.

Superoxide Anion Assay

U937 cells were primed by human interferon-γ (40 units/mL) for 5 days, and the cell suspension was equally divided into 5.0×10^5 cells/well in a 96-well plate. Next, we stimulated the cells by adding the reaction components (phorbol-12-myristate-13-acetate, enhancer solution, luminol solution, and buffer). BA-CeNPs (50 or 100 μmol/L, n=4 each) or vehicle (n=4) were administered at the beginning of the assay. The luminescence was measured every 5 minutes for 4 hours with a microplate reader (SpectraMax M5, Molecular Devices LLC, Sunnyvale, CA).

Dichlorodihydrofluorescein Diacetate Assay

RAW264.7 cells (2.0×10^6 cells/well) were stimulated with 100 μmol/L hemin, a toxic breakdown product of hemoglobin, and treated with BA-CeNPs (50, 100, 250, or 500 μmol/L; n=3 in each) or vehicle (n=3). After stimulation, the cells were washed and suspended in 1 mL of PBS (37°C) with 2 μmol/L dichlorodihydrofluorescein diacetate and incubated for 20 mins at 37°C. Propidium iodide (3 μmol/L) was used to stain ruptured cells. We measured the mean intensity of dichlorodihydrofluorescein fluorescence of propidium iodide negative cells by flow cytometry (BD FACSCalibur, BD Bioscience), using a 488-nm laser for excitation and a 535-nm laser for detection.

Lactate Dehydrogenase Assay

RAW264.7 cells were seeded in 96-well plates (3×10^4 cells/well) and grown in culture medium for 24 hours at 37°C. The culture medium was changed to phenol red-free DMEM containing 1% fetal bovine serum 30 minutes before the assay to reduce hemin binding to albumin. The total lactate dehydrogenase (LDH) contents were measured after exposure to 2% Triton X-100. To determine the maximal toxic condition, we treated hemin to the culture media with different concentrations (0, 20, 40, 60, 80, 100 μmol/L; n=4 each) for 6 hours or different duration of 100 μmol/L hemin (0, 2, 4, and 6 hours; n=4 each), and the LDH assay was performed. To investigate the protective effects, BA-CeNPs (50 or 100 μmol/L; n=4 each) or vehicle (n=4) were treated with 100 μmol/L hemin for 6 hours and performed the LDH assay.

Transmission Electron Microscopy Examination of Cell Morphology

Samples were embedded in PolyBed 812 and ultrathin sections (65 nm) stained with 6% uranyl acetate and 4% lead citrate were observed in a transmission electron microscopy (JEM-1400, JEOL) at 80 kV.

In Vitro Terminal Deoxynucleotidyl Transferase dUTP Nick End Labeling

RAW264.7 cells were prepared in 8-well chamber slides (2×10^5 cells/chamber). The cells were stimulated with 100 μmol/L of hemin and treated with BA-CeNPs (50 or 100 μmol/L; n=4 each) or vehicle (n=4). After 6 hours, the cells were fixed with 4% paraformaldehyde and permeabilized by 0.1% Triton X-100 in 0.1% sodium citrate for 2 minutes at 2 to 8°C. Terminal deoxynucleotidyl transferase dUTP nick end labeling (TUNEL) reaction mixture (50 μL; Roche, Penzberg, Germany) was added to the solution and the cells were counter-stained with 4,6-diamidino-2-phenylindole. TUNEL-positive cells were counted and averaged in 4 randomly selected fields at 200× magnification per chamber (Leica DM5500B, Leica Biosystems Inc).

Animal SAH Model: Endovascular Middle Cerebral Artery Perforation

All animal experiments were approved by Institutional Animal Care and Use Committee of Seoul National University and performed according to the institutional guideline for animal research. A total of 155 male Sprague-Dawley rats weighing 230 to 270 g were used. The endovascular perforation model of SAH in rats was performed as previously described with slight modification.[23] Rats were anesthetized with 2.5% isoflurane. A sharpened 4-0 monofilament was inserted into left internal carotid artery from left external carotid artery stump and perforated the bifurcation of the left and middle cerebral artery. Sham-operated rats underwent the same procedure except the insertion of the suture. Representative data of physiological variables of the model are provided in Figure I in the online-only Data Supplement.

The Design of Animal Experiments

A single dose of BA-CeNPs (0.5 mg Ce/kg) or the control (the same volume of saline) was injected via tail vein at an hour after SAH with randomization using the computer-generated schedules. Allocation concealment and blind assessment of outcome was achieved by having an independent investigator prepare drug individually and label it according to the randomization schedule. The study consisted of 2 sets of experiments. Experiment 1: the rats were divided randomly into the following groups: sham-operated (n=18), SAH+saline (n=35), and SAH+BA-CeNPs (n=35). SAH grades, neurological scores, and brain water content were measured at 24 and 72 hours after SAH. A priori exclusion criteria were early death before injection, death before time points of analysis, or incomplete modeling because of low-SAH grades. Fluorescent immunostaining was performed at 72 hours after SAH. Experiment II: the rats were divided randomly into the following groups: SAH+saline (n=25) and SAH+BA-CeNPs (n=25). A priori exclusion criterion was early death before BA-CeNPs or saline injection. Mortality was assessed daily for 14 days after SAH. Serial neurological score was evaluated at 1, 3, 5, 10, and 14 days after SAH.

Brain Distribution of BA-CeNPs in SAH Model

After 1 hour of SAH induction, 0.5 mg Ce/kg of rhodamine isothiocyanate labeled BA-CeNPs were administered to the rats via the tail vein; 4 of 10 animals died within 1 hour and 2 of 10 animals died before the analysis. At 24 or 72 hours after SAH, the rats (n=2 each) were euthanized and the brains (40 μm, coronal section) were examined by confocal microscopy (Leica DM5500B, Leica Biosystems Inc). A 3-dimensional contour plots of kernel density estimate of the fluorescence signals was conducted using MATLAB R2017a (MathWorks, Inc, Natick, MA).

SAH Grade

The SAH grades were evaluated by use of the grading scale measuring the bleeding severity.[24] Briefly, after animals were euthanized and the brains were removed, the basal cistern was divided into 6 segments. Each segment was scored from 0 to 3 by the amount of subarachnoid blood and a total score was calculated ranging from 0 to 18 after adding the scores from all segments. Rats with mild SAH (a total score of ≤7) were excluded from the study.

Assessment of Neurological Outcome After SAH

Neurological scores were evaluated according to the scoring system of modified Garcia test consisting of 6 parameters (spontaneous activity, symmetry in the movement of all 4 limbs, forepaw outstretching, climbing, body proprioception, and response to vibrissae stimulation).[24,25]

Measurement of Neuronal Cell Death and Macrophage Infiltration After SAH

The coronal sections of the brain of 10 μm thick at the level of bregma-2 mm were cut on a cryostat and mounted on poly-L-lysine-coated slides. To estimate neuronal cell death, we immunostained the brain sections with antineuronal nuclei antibody (1:100; no. 12943S, Cell Signaling Technology, Danvers, MS) as the primary antibody and Alexa Fluor 555 goat anti-rabbit IgG (1:200; A21428, Invitrogen, Carlsbad, CA) as the secondary antibody. Next, we stained the sections with TUNEL-staining kit (Promega, Madison, WI). To label macrophages, CD68 (ab125212, Abcam, Cambridge, MA) was used as the primary antibody and Alexa Fluor 488 goat anti-rabbit IgG (A11008, Invitrogen) as the secondary antibody. The TUNEL-positive neurons or CD68-positive cells were counted in the ipsilateral (left) basal cortex in 6 fields per animal at 200× magnification, and data were expressed as the number of TUNEL-positive neurons/mm^2 and CD68-positive cells/mm^2.

Measurement of Brain Edema in SAH

After euthanasia, the brains were divided into left and right hemispheres, cerebellum, and brain stem. Each part was immediately weighed on an electronic analytical balance to obtain the wet weight. Then, each part was dried in a gravity oven at 105°C for 72 hours and weighed to obtain the dry weight. The water content was calculated using the following formula: ([wet weight−dry weight]/wet weight)×100.[26]

Statistical Analysis

Data are expressed as mean and SEM. Superoxide anion assay was analyzed with 2-way ANOVA with Tukey multiple comparisons test. Survival curves were compared with log-rank test. Neurological scores were compared using unpaired *t* test. All other data were analyzed by 1-way ANOVA with Tukey multiple comparisons test. A *P* value of <0.05 was defined statistically significant. All statistical analyses were performed using GraphPad Prism version 7.0a (GraphPad Software, San Diego, CA)

Results

Characteristics of BA-CeNPs

We synthesized CeNPs totally in aqueous phase using aminocaproic acid as previously described,[27] and modified reaction conditions to achieve 3 nm size and a high Ce^{3+} proportion. Transelectron microscopic imaging showed 3 nm discrete CeNPs with lattice planes (Figure 1A). The wide-angle X-ray diffraction spectrum showed BA-CeNPs had a combination of CeO_2 (JCPDS card no. 34–0394) and Ce_2O_3 (JCPDS card no. 78–0484) peak patterns (Figure 1B). X-ray photoelectron spectroscopy spectra showed the mixed oxidation states of Ce^{3+} and Ce^{4+} and the ratio was 57% to 43% (Figure 1C). Thermogravimetric analysis showed the mass ratio of aminocaproic acid to cerium in BA-CeNPs was 2.434: 1 (Figure II in the online-only Data Supplement). To increase biocompatibility, we induced the formation of covalent bonds between the amine groups of aminocaproic acid and the succinimidyl groups of polyethylene glycol (Figure 1D).

ROS Scavenging and Cytoprotective Effect of BA-CeNPs

To investigate macrophage uptake of BA-CeNPs, we performed fluorescence-activated cell-sorting study using fluorescent dye-conjugated BA-CeNPs. The cellular uptake increased in a dose- and time-dependent manner (Figure III in the online-only Data Supplement). In superoxide anion assay, BA-CeNPs significantly reduced the level of superoxide anions generated in the cells stimulated by phorbol-12-myristate-13-acetate (Figure 2A). BA-CeNPs decreased

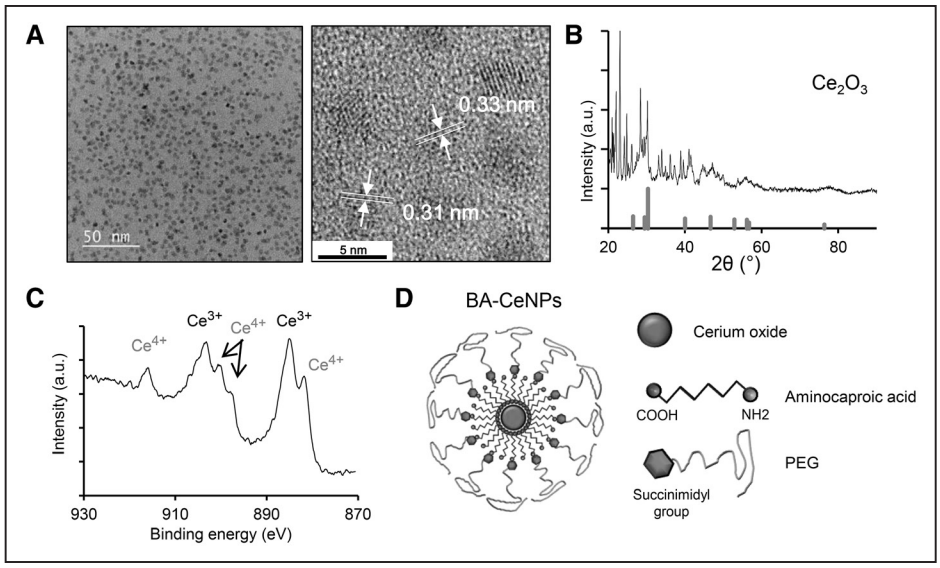

Figure 1. Physicochemical characteristics of biocompatible, aminocaproic acid-ceria nanoparticles (BA-CeNPs). **A**, Transmission electron microscopy (TEM) images of BA-CeNPs. **B**, X-ray diffraction spectrum of BA-CeNPs. **C**, X-ray photoelectron spectroscopy analysis. **D**, Schematic representation of BA-CeNPs. PEG indicates polyethylene glycol.

the level of total intracellular ROS measured with dichlorodihydrofluorescein diacetate in hemin-stimulated RAW264.7 cells as compared with the control (Figure 2B). Hemin (ferriprotoporphyrin IX chloride), an oxidized form of the heme of blood, is highly cytotoxic through massive ROS generation and leads to inflammation by stimulating macrophages.[28] We treated macrophages with increasing concentrations and time of hemin to determine the degree of cytotoxicity. Hemin was dose- and time-dependently cytotoxic to macrophages, as determined by the release of LDH in the supernatants of

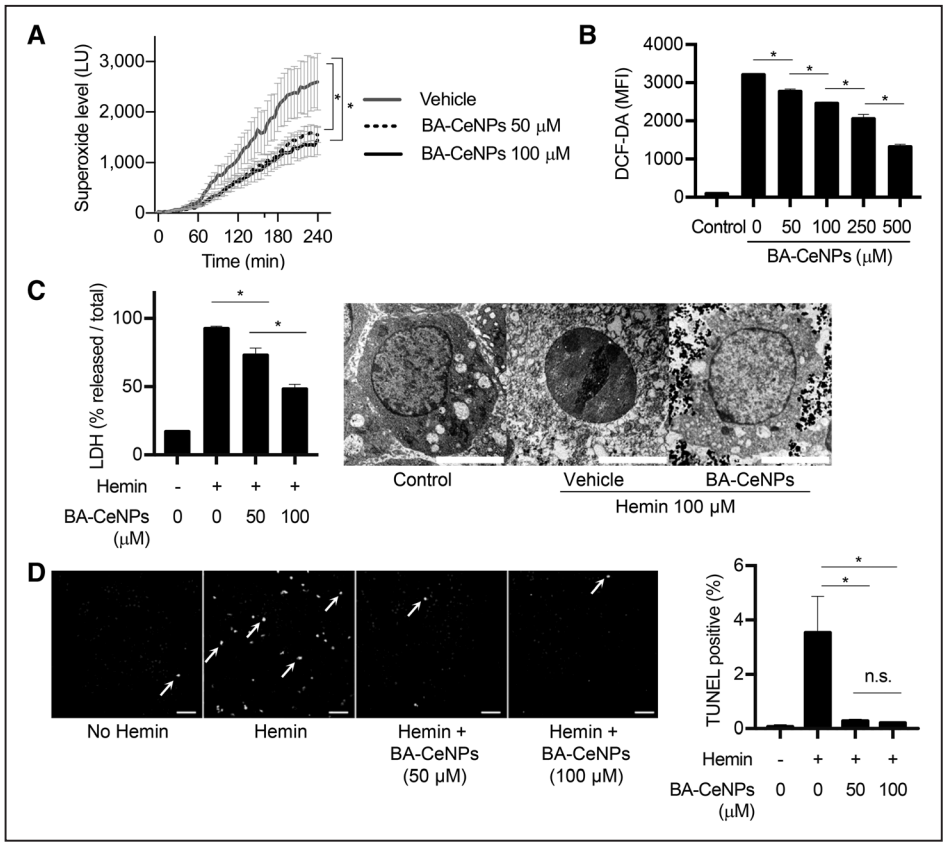

Figure 2. Effects of biocompatible, aminocaproic acid-ceria nanoparticles (BA-CeNPs) treatment in vitro hemin stimulation model. **A**, Superoxide anion assay. **B**, Dichlorodihydrofluorescein diacetate (DCF-DA) assay for intracellular reactive oxygen species (ROS) measurement; **C**, Lactate dehydrogenase (LDH) assay and transmission electron microscopic images. Scale bar, 5 μm. **D**, Terminal deoxynucleotidyl transferase dUTP nick end labeling (TUNEL; arrow) for DNA fragmentation. *P<0.05. LU indicates luminescence unit; and MFI, mean fluorescence intensity.

cells, which peaked at 6 hours and 100 μmol/L (Figure IV in the online-only Data Supplement). However, BA-CeNPs treatment protected macrophages from hemin-induced cell death, as determined by measuring LDH in the supernatant and transmission electron microscopy findings such as plasma membrane rupture, excessive vacuole formation, and nuclear condensation (Figure 2C). DNA fragmentation determined by TUNEL-positive nuclei were also reduced with BA-CeNPs treatment (Figure 2D).

Distribution of BA-CeNPs in the SAH Brain

We conducted an experiment to determine that BA-CeNPs can be distributed in the brain when intravenously injected into a rodent SAH model. Rhodamine isothiocyanate labeled BA-CeNPs at 72 hours after SAH were more distributed in the ipsilateral hemisphere where the artery was ruptured than in the contralateral hemisphere (Figure 3A and B). About cellular distribution, rhodamine isothiocyanate labeled BA-CeNPs reached the cytoplasm of neuronal cells and macrophages in the brain with SAH (Figure 3C and 3D).

Neuroprotective and Anti-Inflammatory Effects of BA-CeNPs

To investigate therapeutic effects of BA-CeNPs in SAH model, we performed 70 SAH and 18 sham surgeries. A total of 37 animals were excluded by a priori criteria: 18 animals died before BA-CeNPs or saline injection, 13 animals were injected but died before the analysis (9 in the saline group; 4 in the BA-CeNPs group), and 6 animals had SAH grade ≤7 (2 in the saline group; 4 in the BA-CeNPs group; Figure 4A). We assessed whether BA-CeNPs could reduce brain injuries after SAH by reducing the magnitude of neuronal death and macrophage infiltration. The SAH grades were comparable in the BA-CeNPs group and the saline group at 24 and 72 hours (Figure 5A). Neuronal cell death at the basal cortex increased to 246.9±14.1 per mm^2 after 72 hours of induction of SAH, but treatment with BA-CeNPs reduced it to 2.2±1.3 per mm^2 (P value <0.001; Figure 5B). While CD68-positive macrophage infiltrated into the basal cortex increased to 368.7±30.1 per mm^2 after 72 hours of induction of SAH, but treatment with BA-CeNPs also reduced it to 144.3±70.7 per mm^2 (P value=0.008; Figure 5C). Treatment with BA-CeNPs resulted in a significant decrease in brain water content in the ipsilateral hemisphere and cerebellum at 24 and 72 hours (Figure 5D).

Improved Survival and Neurological Outcome by BA-CeNPs

As a randomized animal trial of BA-CeNPs for survival and neurological outcomes in SAH model, we performed 50 SAH surgeries and assigned them to BA-CeNPs (n=25) and saline (n=25) injection. Fourteen animals died before BA-CeNPs or saline injection, and 36 animals were injected (n=19, the saline group; n=17, the BA-CeNPs group) and followed-up for 14 days for assessment of mortality and neurological outcome

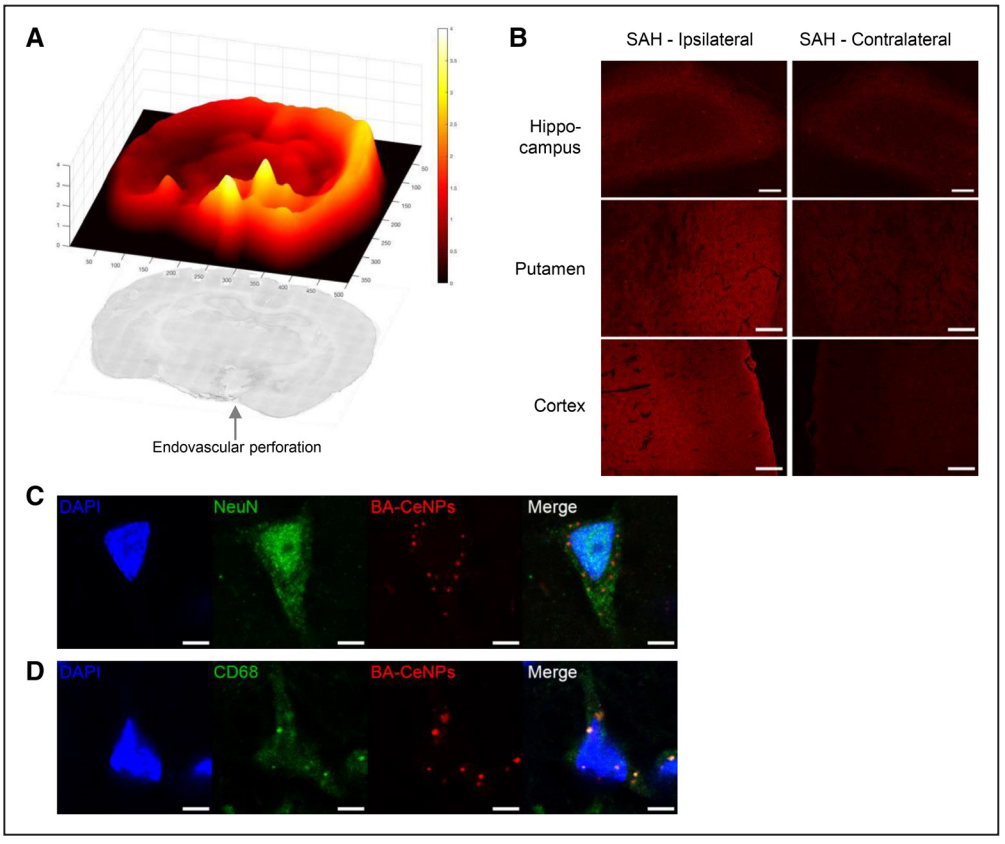

Figure 3. Distribution of biocompatible, aminocaproic acid-ceria nanoparticles (BA-CeNPs) in the brain after subarachnoid hemorrhage. **A**, Three-dimensional kernel density plot of rhodamine isothiocyanate (RITC) labeled BA-CeNPs in the brain at 72 h after subarachnoid hemorrhage (SAH) induction. **B**, Regional distribution of RITC-BA-CeNPs in hippocampal, putaminal and cortical area of SAH. scale bar, 200 μm. **C** and **D**, Intracellular uptake of RITC labeled BA-CeNPs in (**C**) neuronal cell and (**D**) active macrophages. Scale bar, 5 μm.

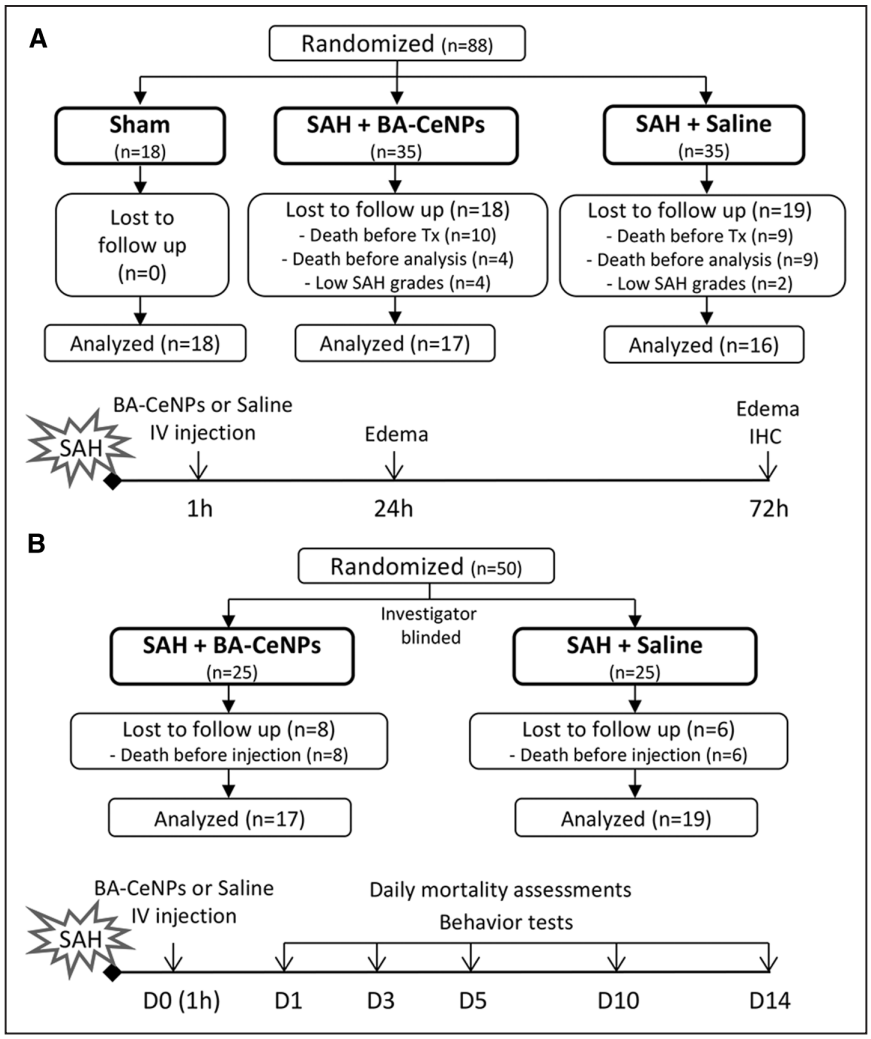

Figure 4. Experimental designs. **A**, Experiment 1: measurement of brain edema, macrophage infiltration, and neuronal deaths. **B**, Experiment 2: a randomized, investigator-blinded animal trial of biocompatible, aminocaproic acid-ceria nanoparticles (BA-CeNPs) for mortality and neurological outcomes. IV indicates intravenous; and SAH; subarachnoid hemorrhage.

(Figure 4B). BA-CeNPs treatment after SAH showed higher survival rate (P value <0.001 by log-rank test) compared with the saline-treated group (Figure 6A). There was a significant survival difference from the early period (survival rate at day 3, 100% in the BA-CeNPs group versus 47.4% in the saline group). This gap gradually increased during the subacute period, with the largest difference at day 14 (survival rate at day 14, 88.2% in the BA-CeNPs group vs. 21.1% in the saline group). Neurological scores of survivors were higher in the BA-CeNPs group than in the saline group from the early phase (modified Garcia score at day 3, 12.1±0.5 in the BA-CeNPs group versus 4.4±0.5 in the saline group), and there is no significant difference between each time points (Figure 6B; Table I in the online-only Data Supplement).

Discussions

BA-CeNPs reduced mortality and improved neurological outcome in the SAH model because of the powerful ROS scavenging activity of BA-CeNPs and subsequent neuroprotective and anti-inflammatory effects. In SAH, acute global cerebral ischemia is induced by massive bleeding into the subarachnoid space leading to increased intracranial pressure and reduced cerebral perfusion. The initial global ischemia provokes a burst generation of ROS in the brain that plays a central role in the early neuronal cell deaths in SAH.[28–30] In the SAH animal model, the capacity of the endogenous antioxidant system is depleted within the first hour after SAH development.[31] The superfluous formation of ROS paralyzing the intrinsic antioxidant systems has also been demonstrated in the brain after SAH in humans.[32–34] Moreover, blood clot itself generates a large amount of ROS in the subarachnoid space via autoxidation, the Fenton reaction of heme, and toxic effects of thrombin, which evokes massive neuroinflammation and subsequent brain injuries.[15,16,35] The neuroprotection by CeNPs can be exerted by directly reducing oxidative damages to neuronal cells induced by ischemia and indirectly suppressing highly destructive neuroinflammation after SAH. From these mechanisms, CeNPs played a therapeutic role as an extrinsic antioxidant system in the milieu of overflowing ROS in SAH.

For diseases characterized by excessive ROS formation within hours after onset such as SAH, a novel entity of ROS scavenger with high potency and instant onset is required. Commercial antioxidant drugs or enzymes have not been successful because of the low potency, which could be overcome by using nanoenzymes of enhanced efficacy. Ceria nanoparticle can be a promising candidate of free radical scavenging therapy because of its potent, self-regenerating, and versatile antioxidative activities.[36] The redox cycling between Ce^{3+}

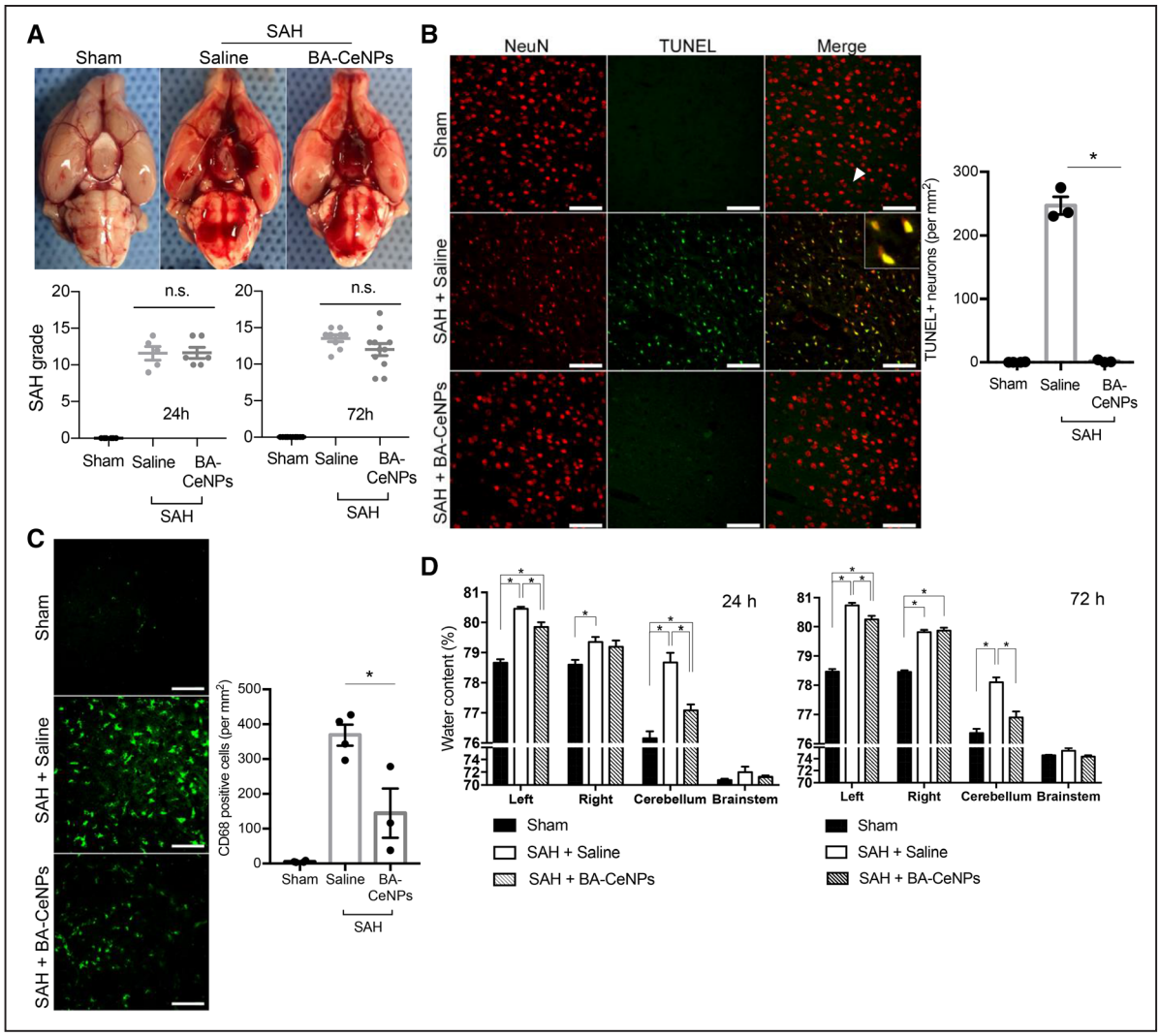

Figure 5. Therapeutic effects of biocompatible, aminocaproic acid-ceria nanoparticles (BA-CeNPs) in animal subarachnoid hemorrhage (SAH) models. **A**, Comparison of the amount of SAH between sham, saline-treated, and BA-CeNPs treated groups. **B**, Evaluation of neuronal cell death in the basal cortex at 72 h, using colocalization of neuronal nuclei (NeuN) and terminal deoxynucleotidyl transferase dUTP nick end labeling (TUNEL). scale bar, 100 μm. **C**, Evaluation of CD68-positive macrophage infiltration in the basal cortex at 72 h. Scale bar, 100 μm. **D**, Effect of BA-CeNPs treatment on brain edema measured at 24 and 72 h after SAH. Mean±SEM. *P value <0.05.

and Ce^{4+} ion on the surface of ceria nanoparticle enables it to rapidly scavenge a large amount of ROS.[37] Because of their high surface-to-volume ratio, CeNPs has many active sites per single particle, eliminating a variety of ROS-including superoxide, hydrogen peroxide, and hydroxyl radicals.[18,20,21] These characteristics allow severe strokes such as SAH to become the ideal venue of translating CeNPs into free radical scavenging therapy.

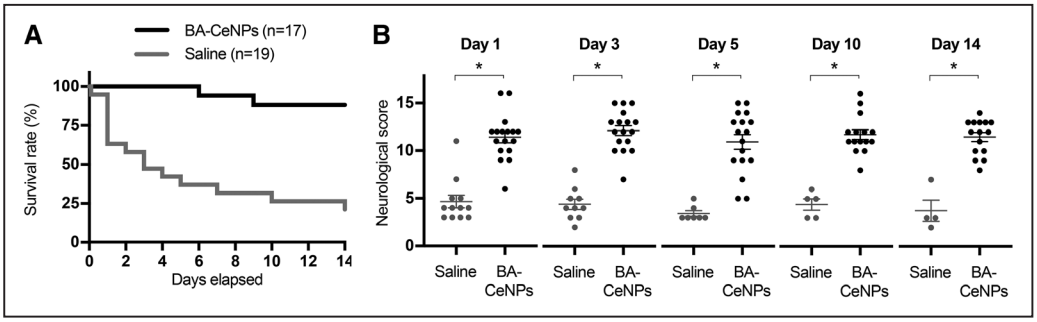

Figure 6. A randomized, investigator-blinded trial of biocompatible, aminocaproic acid-ceria nanoparticles (BA-CeNPs) in subarachnoid hemorrhage (SAH) model for survival and neurological outcomes. **A**, Survival curve of SAH models during 14 d after the BA-CeNPs or saline treatment. P<0.001 by log-rank test. **B**, Neurological scores (modified Garcia score; the best score is 18 points) of the survivors at day 1, 3, 5, 10, and 14 after BA-CeNPs or saline treatment. *P<0.001.

We chose aminocaproic acid as a surface modifier for the following reasons. Since CeNP was originally developed for industrial purpose, a synthetic method using biocompatible materials without toxic-organic solvents is required to ensure safety for human applications. Aminocaproic acid allows synthesis of monocrystalline CeNPs in aqueous solution without phase transfer from organic solvents.[27] The resulting high Ce^{3+} to Ce^{4+} ratio of BA-CeNPs represents more potent superoxide anion and hydroxyl radical scavenging activities. Although aminocaproic acid may be used to reduce the risk of early aneurysm rebleeding in selected clinical cases, the severity of SAH was not different between BA-CeNPs or saline-treated group in our study. This may be because the aminocaproic acid content in BA-CeNPs was much lower than the hemostatic dose or was administered after the arterial bleeding finished. Although endovascular perforation model causes arterial bleeding that closely mimics the mechanisms of human SAH, varying SAH severity in the model can lead to bias, which mandated randomization and allocation concealment in our study.

Conclusions

BA-CeNPs can protect the brain against SAH, the most devastating type of stroke, via prominent and versatile ROS scavenging effects. Using aminocaproic acid as a surface modifier, BA-CeNPs can be synthesized totally in aqueous phase without toxic-organic solvent. A high Ce^{3+} to Ce^{4+} ratio of BA-CeNPs represents more potent ROS scavenging activities and neuroprotective effects in SAH. Despite advancement of aneurysm repair to prevent rebleeding, mortality and disability caused by SAH are still high because of lack of effective therapy targeting secondary brain injuries in SAH. The promising results of this report suggest the potential of free radical scavenging therapy using CeNPs for SAH and may require further preclinical tests, including pharmacokinetics and chronic toxicity.

Acknowledgments

Dr Jeong received 2018 Stroke Basic Science Award at International Stroke Conference from the American Heart Association/American Stroke Association for this work.

Sources of Funding

This research was supported by the Korea Health Technology R&D Project through the Korea Health Industry Development Institute (KHIDI) funded by the Ministry of Health & Welfare, Republic of Korea (HI17C0076), and the Basic Science Research Program through the National Research Foundation of Korea (NRF) funded by the Ministry of Science and ICT (NRF-2018R1A2A2A05022369).

Disclosures

None.

References

1. Bonita R, Thomson S. Subarachnoid hemorrhage: epidemiology, diagnosis, management, and outcome. *Stroke*. 1985;16:591–594.
2. Schievink WI, Wijdicks EF, Parisi JE, Piepgras DG, Whisnant JP. Sudden death from aneurysmal subarachnoid hemorrhage. *Neurology*. 1995;45:871–874.
3. Johnston SC, Selvin S, Gress DR. The burden, trends, and demographics of mortality from subarachnoid hemorrhage. *Neurology*. 1998;50:1413–1418.
4. Connolly ES Jr, Rabinstein AA, Carhuapoma JR, Derdeyn CP, Dion J, Higashida RT, et al; American Heart Association Stroke Council; Council on Cardiovascular Radiology and Intervention; Council on Cardiovascular Nursing; Council on Cardiovascular Surgery and Anesthesia; Council on Clinical Cardiology. Guidelines for the management of aneurysmal subarachnoid hemorrhage: a guideline for healthcare professionals from the American Heart Association/American Stroke Association. *Stroke*. 2012;43:1711–1737. doi: 10.1161/STR.0b013e3182587839
5. Dorhout Mees S, Rinkel GJE, Feigin VL, Algra A, van den Bergh WM, Vermeulen M, et al. Calcium antagonists for aneurysmal subarachnoid haemorrhage. *Cochrane Database Syst Rev*. 2007;(3):CD000277.
6. Prunell GF, Svendgaard NA, Alkass K, Mathiesen T. Delayed cell death related to acute cerebral blood flow changes following subarachnoid hemorrhage in the rat brain. *J Neurosurg*. 2005;102:1046–1054. doi: 10.3171/jns.2005.102.6.1046
7. Cahill J, Calvert JW, Solaroglu I, Zhang JH. Vasospasm and p53-induced apoptosis in an experimental model of subarachnoid hemorrhage. *Stroke*. 2006;37:1868–1874. doi: 10.1161/01.STR.0000226995.27230.96
8. Park S, Yamaguchi M, Zhou C, Calvert JW, Tang J, Zhang JH. Neurovascular protection reduces early brain injury after subarachnoid hemorrhage. *Stroke*. 2004;35:2412–2417. doi: 10.1161/01.STR.0000141162.29864.e9
9. Friedrich V, Flores R, Sehba FA. Cell death starts early after subarachnoid hemorrhage. *Neurosci Lett*. 2012;512:6–11. doi: 10.1016/j.neulet.2012.01.036
10. Fujii M, Yan J, Rolland WB, Soejima Y, Caner B, Zhang JH. Early brain injury, an evolving frontier in subarachnoid hemorrhage research. *Transl Stroke Res*. 2013;4:432–446. doi: 10.1007/s12975-013-0257-2
11. Sehba FA, Bederson JB. Mechanisms of acute brain injury after subarachnoid hemorrhage. *Neurol Res*. 2006;28:381–398. doi: 10.1179/016164106X114991
12. Cahill J, Cahill WJ, Calvert JW, Calvert JH, Zhang JH. Mechanisms of early brain injury after subarachnoid hemorrhage. *J Cereb Blood Flow Metab*. 2006;26:1341–1353. doi: 10.1038/sj.jcbfm.9600283
13. Samuelsson C, Hillered L, Enblad P, Ronne-Engström E. Microdialysis patterns in subarachnoid hemorrhage patients with focus on ischemic events and brain interstitial glutamine levels. *Acta Neurochir (Wien)*. 2009;151:437–446; discussion 446. doi: 10.1007/s00701-009-0265-x
14. Enblad P, Valtysson J, Andersson J, Lilja A, Valind S, Antoni G, et al. Simultaneous intracerebral microdialysis and positron emission tomography in the detection of ischemia in patients with subarachnoid hemorrhage. *J Cereb Blood Flow Metab*. 1996;16:637–644. doi: 10.1097/00004647-199607000-00014
15. Fortes GB, Alves LS, de Oliveira R, Dutra FF, Rodrigues D, Fernandez PL, et al. Heme induces programmed necrosis on macrophages through autocrine TNF and ROS production. *Blood*. 2012;119:2368–2375. doi: 10.1182/blood-2011-08-375303
16. Rifkind JM, Mohanty JG, Nagababu E. The pathophysiology of extracellular hemoglobin associated with enhanced oxidative reactions. *Front physiol*. 2015;5:500. doi: 10.3389/fphys.2014.00500
17. Singh S, Dosani T, Karakoti AS, Kumar A, Seal S, Self WT. A phosphate-dependent shift in redox state of cerium oxide nanoparticles and its effects on catalytic properties. *Biomaterials*. 2011;32:6745–6753. doi: 10.1016/j.biomaterials.2011.05.073
18. Pirmohamed T, Dowding JM, Singh S, Wasserman B, Heckert E, Karakoti AS, et al. Nanoceria exhibit redox state-dependent catalase mimetic activity. *Chem Commun (Camb)*. 2010;46:2736–2738. doi: 10.1039/b922024k
19. Xu C, Qu X. Cerium oxide nanoparticle: a remarkably versatile rare earth nanomaterial for biological applications. *NPG Asia Mater*. 2014;6:e90.
20. Korsvik C, Patil S, Seal S, Self WT. Superoxide dismutase mimetic properties exhibited by vacancy engineered ceria nanoparticles. *Chem Commun*. 2007;(10):1056–1058
21. Xue Y, Luan Q, Yang D, Yao X, Zhou K. Direct evidence for hydroxyl radical scavenging activity of cerium oxide nanoparticles. *J Phys Chem C*. 2011;115:4433–4438.
22. Reed K, Cormack A, Kulkarni A, Mayton M, Sayle D, Klaessig F, et al. Exploring the properties and applications of nanoceria: is there still plenty of room at the bottom? *Environ Sci Nano*. 2014;1:390–405.
23. Bederson JB, Germano IM, Guarino L. Cortical blood flow and cerebral perfusion pressure in a new noncraniotomy model of subarachnoid hemorrhage in the rat. *Stroke*. 1995;26:1086–1091; discussion 1091.
24. Sugawara T, Ayer R, Jadhav V, Zhang JH. A new grading system evaluating bleeding scale in filament perforation subarachnoid

hemorrhage rat model. *J Neurosci Methods*. 2008;167:327–334. doi: 10.1016/j.jneumeth.2007.08.004
25. Garcia JH, Liu KF, Ho KL. Neuronal necrosis after middle cerebral artery occlusion in Wistar rats progresses at different time intervals in the caudoputamen and the cortex. *Stroke*. 1995;26:636–642; discussion 643.
26. Kim CK, Ryu WS, Choi IY, Kim YJ, Rim D, Kim BJ, et al. Detrimental effects of leptin on intracerebral hemorrhage via the STAT3 signal pathway. *J Cereb Blood Flow Metab*. 2013;33:944–953. doi: 10.1038/jcbfm.2013.35
27. Yu T, Lim B, Xia Y. Aqueous-phase synthesis of single-crystal ceria nanosheets. *Angew Chem Int Ed Engl*. 2010;49:4484–4487.
28. Lee JY, Keep RF, He Y, Sagher O, Hua Y, Xi G. Hemoglobin and iron handling in brain after subarachnoid hemorrhage and the effect of deferoxamine on early brain injury. *J Cereb Blood Flow Metab*. 2010;30:1793–1803. doi: 10.1038/jcbfm.2010.137
29. Matz P, Weinstein P, States B, Honkaniemi J, Sharp FR. Subarachnoid injections of lysed blood induce the hsp70 stress gene and produce DNA fragmentation in focal areas of the rat brain. *Stroke*. 1996;27:504–512; discussion 513.
30. Arai T, Takeyama N, Tanaka T. Glutathione monoethyl ester and inhibition of the oxyhemoglobin-induced increase in cytosolic calcium in cultured smooth-muscle cells. *J Neurosurg*. 1999;90:527–532. doi: 10.3171/jns.1999.90.3.0527
31. Marzatico F, Gaetani P, Cafè C, Spanu G, Rodriguez y Baena R. Antioxidant enzymatic activities after experimental subarachnoid hemorrhage in rats. *Acta Neurol Scand*. 1993;87:62–66.
32. Gaetani P, Pasqualin A, Rodriguez y Baena R, Borasio E, Marzatico F. Oxidative stress in the human brain after subarachnoid hemorrhage. *J Neurosurg*. 1998;89:748–754. doi: 10.3171/jns.1998.89.5.0748
33. Kaynar MY, Tanriverdi T, Kemerdere R, Atukeren P, Gumustas K. Cerebrospinal fluid superoxide dismutase and serum malondialdehyde levels in patients with aneurysmal subarachnoid hemorrhage: preliminary results. *Neurol Res*. 2005;27:562–567. doi: 10.1179/016164105X17288
34. Marzatico F, Gaetani P, Tartara F, Bertorelli L, Feletti F, Adinolfi D, et al. Antioxidant status and alpha1-antiproteinase activity in subarachnoid hemorrhage patients. *Life Sci*. 1998;63:821–826.
35. Sugawara T, Jadhav V, Ayer R, Chen W, Suzuki H, Zhang JH. Thrombin inhibition by argatroban ameliorates early brain injury and improves neurological outcomes after experimental subarachnoid hemorrhage in rats. *Stroke*. 2009;40:1530–1532. doi: 10.1161/STROKEAHA.108.531699
36. Nelson BC, Johnson ME, Walker ML, Riley KR, Sims CM. Antioxidant cerium oxide nanoparticles in biology and medicine. *Antioxidants*. 2016;5:E15. doi: 10.3390/antiox5020015
37. Karakoti A, Singh S, Dowding JM, Seal S, Self WT. Redox-active radical scavenging nanomaterials. *Chem Soc Rev*. 2010;39:4422–4432. doi: 10.1039/b919677n